CORONAE OF COOL STARS

M. Güdel [a]

[a]Paul Scherrer Institut, Würenlingen and Villigen, CH-5232 Villigen PSI, Switzerland

High-resolution X-ray spectroscopy from *XMM-Newton* and *Chandra* has given new access to a number of physical processes occurring in cool star atmospheres. The origin of the observed energy is in the center of current debates, although there is little doubt that the magnetic fields confining the plasma are themselves responsible for the energy release. Density diagnostics from X-ray spectra is used to derive pressures, emitting masses and volumes and therefore the thermal energy in the plasma. The composition of stellar coronae reveals a number of anomalies in particular in magnetically active stars that are unexplained. Spectroscopy is also a valuable tool for measuring mass flows and Doppler motions in binary systems. Despite the large information content in X-ray spectra, numerous caveats due to the complexity of coronae should be considered. The interpretation of stellar coronal spectra should in particular address the statistical properties of coronae, e.g., time-dependent stochastic heating, statistical distributions of densities across the coronal volume, or time- and temperature-dependent composition.

1. Introduction

Considered ideal sources for instrument calibration and examples of thermal line emitters by some, but challenging plasma physical sources of violent energy release by others, magnetized outer atmospheres of cool stars are textbook examples of cosmic high-energy sources in particular for the new generation of X-ray observatories. At first sight, they appear to lack the capacity for surprise now witnessed in research of more "exotic" objects where almost every new high-resolution spectrum is a "first", a new chapter written in the language of spectroscopy. The spectra of stellar coronae were anticipated from high-resolution studies of the solar corona and modeling of stellar spectra taken with low-resolution devices. However, at a more detailed level, up to the present day we do not understand the basic mechanisms that heat stellar coronal plasma three to four orders of magnitude above photospheric levels; the interactions with non-thermal particles with MeV energies are poorly understood; the generation and the interactions of magnetic fields are a matter of debate; the role of magnetic fields in the generation of stellar winds is hardly understood, yet mass loss controls stellar rotation and the dynamo itself; the anomalous composition of coronae and winds keeps secrets related to mass transport and heating; spectroscopically, we have not even understood whether the coronal plasma we observe and interpret with routine is in fact purely thermal!

High-resolution spectroscopy gives access to a number of *physical* issues in stellar coronae, such as processes related to mass accumulation in the corona, the thermal structure, heating processes, etc., issues that are by no means confined to stellar atmospheres but that are favorably studied in such environments. The present paper illuminates a number of basic physical questions, new results, and new problem areas that have emerged in the study of stellar coronae. We are predominantly concerned with high-resolution spectroscopic studies from *XMM-Newton* and *Chandra* but will, in a more cursory way, address a few recent results on main-sequence stars from related investigations using X-ray photometric data. A summary of further recent spectroscopic results specifically from *Chandra* is found in ref. [1] in these proceedings. We follow a chain of events, starting with the primary energy release from magnetic fields and discussing various secondary products.

2. Flares: The Smoking Guns

X-ray astronomy of cool stars is rooted in the question of how and why such stars liberate energy beyond the steady flux of radiation from their photospheres. It became clear in the early days of solar physics that magnetic fields confine the hot, X-ray emitting plasma, but it took another step to establish that the magnetic fields themselves are responsible for actually transporting the energy to coronal heights and release it there. The details of energy transport and release are still only schematically known and very much rely on solar coronal research.

In a standard picture of flare energy release, coronal energy is liberated in regions of magnetic reconnection in the corona. A large fraction of the energy is presumably channeled into acceleration of electrons (and possibly ions) up to MeV energies. Trapped electrons reveal themselves by their radio (R) gyrosynchrotron emission, and as they eventually impact in the stellar chromospheres, optical (O) and nonthermal hard X-ray (HXR, > 10 keV) bursts emerge. These emissions occur promptly and are ideal tracers for the rate of energy input (for radio emission, longer-term trapping of electrons in the corona may have to be considered in some cases). They are therefore expected to occur at the beginning of flares. The kinetic energy deposition in the chromosphere heats plasma and drives ("evaporates") it into the corona, building up the soft X-ray sources; as the cooling time scales of the plasma are usually much longer than the time scales of the initial energy release, the X-rays evolve roughly in proportion with the accumulated energy in the thermal flare plasma. Approximately, we therefore expect

$$L_{\mathrm{R,O,HXR}}(t) \propto \frac{d}{dt} L_{\mathrm{X}}(t), \tag{1}$$

a relation known as the "Neupert Effect" [2] in solar physics. While it does not apply to all solar and stellar flares, its detection in several stellar examples [3–6] provides important evidence for physical mechanisms of energy release in magnetically active stars.

Fig. 1 illustrates a textbook example of a stellar Neupert effect, observed by *XMM-Newton* in the optical and in X-rays [5]. The time derivative of the X-rays closely matches the development of the optical burst. While this does not by itself prove a causal relation between electron acceleration and plasma heating, the kinetic energy provided by the population of high-energy electrons may in fact suffice to heat the observed plasma, as was shown in another example observed simultaneously with *XMM-Newton* (X-rays) and the VLA (at radio wavelengths) [6].

The strong increase in the soft X-ray luminosity during a flare may be related both to an increase in electron density n_e or in volume V, or both, since $L_{\mathrm{X}} \propto n_e^2 V$. To disentangle the degeneracy, explicit measurements of densities using He-like

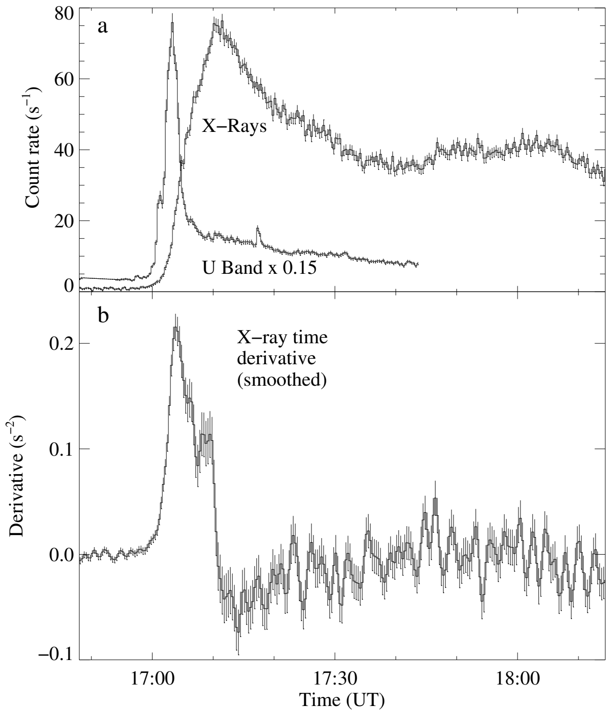

Figure 1. Large flare on Proxima Centauri observed with *XMM-Newton*. The top panel shows the optical U band light curve (early burst) and the X-ray light curve. The bottom panel illustrates the time derivative of the X-ray light curve, which closely resembles the optical light curve (after [5]).

line triplets are available. These consist of three closely separated lines due to the resonance transition (r, 1s^2 $^1S_0$–1s2p $^1P_1$), the intercombination transition (i, 1s^2 $^1S_0$–1s2p $^3P_1$), and the forbidden transition (f, 1s^2 $^1S_0$–1s2s $^3S_1$). The flux ratio $R = f/i$ is density-sensitive (larger ratios for smaller densities [7], and also slightly dependent on the temperature, e.g., ref. [8]; see further below for a discussion of densities in "quiescence").

Fig. 2 illustrates two examples each of the O VII and the Ne IX triplet observed at the primary and secondary peaks and during the decay phase of the flare in Fig. 1. Clearly, a nearly complete suppression of the f line during the flare peaks signals high densities. Inferred values range up to 4×10^{11} cm^{-3}. Because the emission measures are known, the volumes and the thermal energy contents of the plasma can be computed for various times. The results indicate expand-

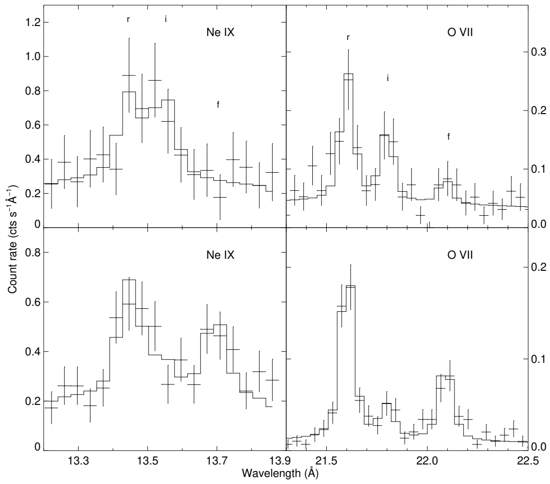

Figure 2. He-like line triplets observed during the flare shown in Fig. 1. Upper panels: during first (17:10 UT) and second (18:00 UT) flare peaks; note the suppressed f line, indicating high densities. Lower panels: Measurements during flare decay, with a larger f/i ratio. The left two panels refer to Ne IX, while the right two panels show the O VII triplets (adapted from [5]).

ing volumes during the flare decay, but thermal energy contents amounting to only a small fraction of the energy eventually radiated by the respective plasma components. This shows that the plasma emitting in the O VII lines (i.e., relatively cool coronal plasma of 1-4 MK) is continuously being replenished during the flare. Apart from the evaporation process itself early in the flare, plasma initially heated to higher temperatures is continuously cooling and thereby becomes a source of O VII emission. Further, though marginal, examples were described in refs. [9,10].

3. A Lot of Smoke: Stochastic Flaring

In solar physics, the concept of "microflaring" has become a central issue for models of coronal heating. The idea is simple: If flares occur at a sufficiently large rate in the corona, they could be the collective source of the observed coronal energy. Previous investigations found that the flare rate is statistically distributed in total flare energy as a power law of the form (e.g., [11])

$$\frac{dN}{dE} = kE^{-\alpha}. \qquad (2)$$

Here, dN is the number of flares (per unit time) with a total energy (thermal or radiated) in the interval $[E, E + dE]$. If $\alpha \geq 2$, then the energy integration (for a given time interval) of Eq. (2) diverges as the lower energy limit $E_1 \to 0$, i.e., arbitrarily large average luminosities can be attained depending on the magnitude of E_1. Recent studies of long time series with the *EUVE* satellite and with *BeppoSAX* indicate a predominance of $\alpha > 2$ for magnetically active stars [12–15]. New studies using *Chandra* support large α values as well [16].

The physical mechanisms at work in low-level flares can be investigated to rather low levels taking advantage of the increased sensitivity of *XMM-Newton* and *Chandra*. A study of the nearest star to the Sun, Proxima Centauri, revealed an almost continual occurrence of flares in the optical U band and in X-rays, many of which follow relation (1) (see Fig. 3). It is therefore conceivable that much of the observed X-ray emission is the result of ongoing chromospheric evaporation rather than of steady radiation from static coronal loops. Such a model explains three features commonly observed in magnetically active stars: i) coronal temperatures that are persistently high; ii) elevated electron densities during "quiescence" (see Sect. 5); iii) high X-ray luminosities, from a large number of high-density magnetic regions induced by frequent evaporative events; iv) quasi-continuous radio emission from the flare-accelerated electrons.

4. Thermal Structure

Early investigations (e.g., [17]) found that the characteristic coronal temperature of a star is correlated with its "activity level" expressed, for example, by the average surface X-ray flux. High-resolution spectroscopy unequivocally supports this view since it gives access to numerous individual temperature-sensitive lines and the continuum. Figure 4 shows examples between the extremes of coronal activity. While the coolest coronae observed radiate predominantly in lines of C, N, and O, the hottest coronae currently known emit predominantly in the bremsstrahlung continuum and in a few lines of highly ionized iron. Detailed spectroscopic analyses are becoming available for an increasing number of individual stars. For examples, we refer to [9,10,18–30], among others.

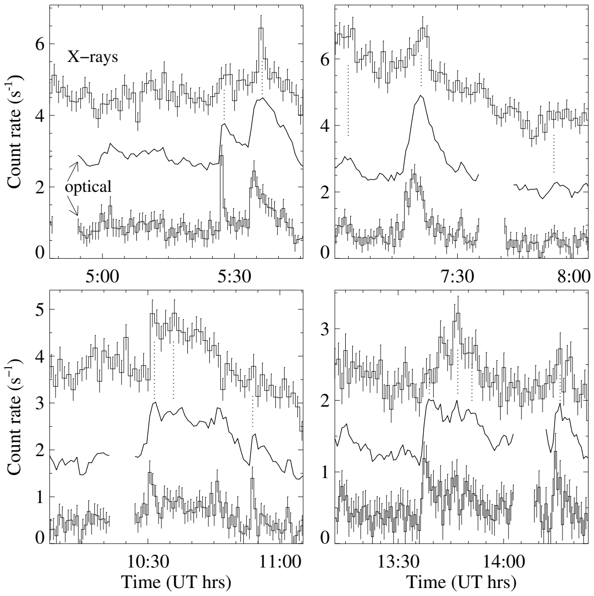

Figure 3. Sequences of small flares observed in the optical U band (lower curves) and the X-rays (upper curves) in Proxima Centauri with *XMM-Newton*. The middle, solid curves are time integrals of the optical curves including an exponential decay term, to illustrate Eq. (1) (adapted from [5]).

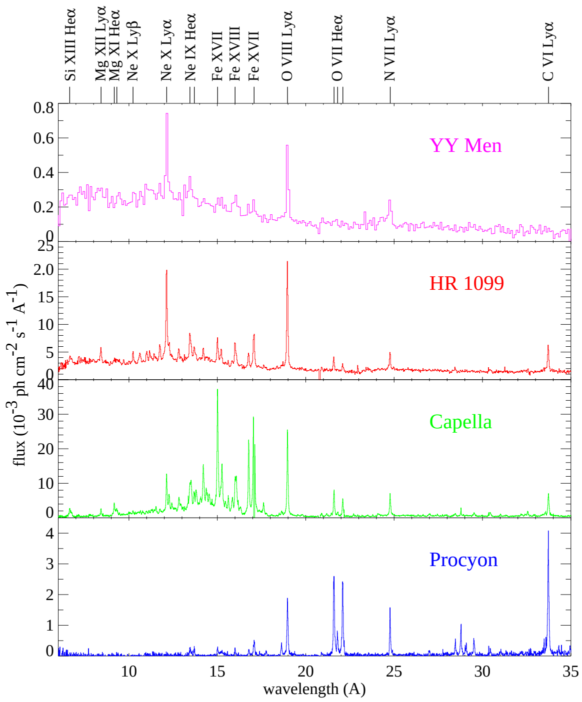

Figure 4. Examples of *XMM-Newton* RGS spectra covering the temperature ranges observed in quiescent stellar coronae. From top to bottom: YY Men, an FK Com-type giant, with a dominant temperature ≈ 30 MK; HR 1099, an RS CVn-type binary with $T_{\rm peak}$ ≈ 10–30 MK; Capella, $T_{\rm peak}$ ≈ 7 MK; and Procyon (F5 IV-V), $T_{\rm peak}$ ≈ 1–2 MK. Note the different continua and line systems.

The cause for the increased efficiency of heating in more active stars is unclear but is obviously related to the higher density of magnetic active regions, or to stronger magnetic fields. One possible model again relates to the presence of a multitude of weak flares since increased coronal temperatures often correlate with increased densities and increased overall luminosities. In that view, stars at high activity levels produce a larger rate of energetic flares. Since flare peak temperatures increase with increasing flare energies (or peak emission measures, see [31]), we expect coronae of more active stars to be hotter on a time average, shifting their emission measure distributions to higher temperatures.

Emission measure distributions of magnetically active stars reveal broad features that often lack significant contributions at temperatures of a few MK [10,21,24,25,29,30]. It appears that the heating mechanism keeps most of the plasma at high temperatures before significant cooling takes effect. The shape of the emission measure distribution itself may contain information of the underlying heating mechanism. For stochastic flares, time-averaged DEMs were calculated by refs. [32] and [15], in both cases suggesting DEMs that fall off steeply toward low temperatures, as suggested by a number of recent observations (e.g., [33]). Contrasting, relatively flat EM distributions were presented for M dwarfs in refs. [34,35].

5. What do Coronal Densities Tell Us?

Energy release in coronal magnetic fields inevitably leads to a coronal density increase, regardless of whether the heating process is steady or transient. If continual chromospheric evaporation is responsible for loading coronal magnetic fields with plasma, then the time-averaged "densities" as measured spectroscopically are expected to be higher in magnetically more active stars.

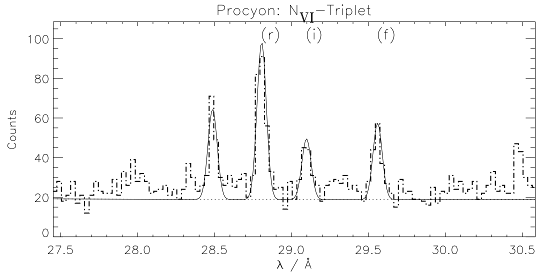

Figure 5. An example of a He-like line triplet of N VI, measured in Procyon with *Chandra* (after [36]).

Refs. [36], [37], and [38] have systematically studied electron densities inferred from the He-like triplets (in particular from C V, N VI, O VII, Ne IX, Mg XI, and Si XIII). Inactive stars such as Capella or Procyon usually show densities around the lower limit accessible by the respective line triplets ($10^9 - 10^{10}$ cm^{-3} for C, N, O). The situation is less clear for magnetically active stars; as long as stars on the main sequence are considered, densities of up to a few times 10^{10} cm^{-3} are inferred for the more active examples [29,30,38]. However, extremely active RS CVn-type binaries often show little indication of densities much above the low-density limit [18,19,21,22,38], with interesting exceptions and trends for higher densities in hotter plasmas (e.g., [10,25]), although some caveats apply, given several problematic line blends [25]. Some caution must also be applied when interpreting f/i ratio measurements from stars of spectral class F and earlier, or when a companion star of such spectral types irradiates a later-type stellar corona in binaries. The f/i ratio may be lowered in these cases by radiative excitation of the $^3P_1$ to the $^3S_1$ level by UV photons. Such cases are described by refs. [36,37].

A peculiarly high apparent density was reported for the classical T Tau star TW Hya [39]. Formally, the He-like triplets imply densities of about 10^{13} cm^{-3}. Such densities are not found in more evolved active binary systems if O VII or Ne IX He-like triplets are used. The authors suggest that such dense plasmas are related to mass accretion columns that produce X-ray emitting shocks near the surface. A strong UV radiation field may "artificially" alter the f/i flux ratio so that the interpretation in terms of densities may be problematic, but since the star's overall photospheric radiation field is irrelevant in this respect, the most likely source for a strong UV radiation field would be the accretion "hot spots" at the funnel-flow footpoints.

What do spectroscopically "measured densities" tell us about the state of a corona, in particular outside obvious flares? Consider a He-like triplet such as the O VII triplet at 22Å. We assume, for the sake of simplicity, an isothermal plasma around the maximum formation temperature of the triplet (there is a slight temperature dependence for the relation between line ratios and inferred densities [8]). For a homogeneous plasma, the flux ratio R between the forbidden line and the intercombination line, f/i, is a function of electron density over typically 3 orders of magnitude in n_e [7,8]. Since the energy flux of each line that is formed in a small plasma volume dV scales with the electron density n_e^2, one needs to integrate the line emission in the f and the i line over a distribution of plasma volumes at different densities across the corona to obtain the total fluxes F and I for the forbidden and the intercombination lines, respectively. The *observed* ratio then is $R_{\rm obs} = F/I$. Since the observed emission is strongly weighted with volumes at high densities, the densities inferred from $R_{\rm obs}$ are biased toward the highest densities occurring in reasonably large volumes. To quantify this effect, we calculate F/I for a corona in which the volume is distributed in density as a power law, viz. $dV/dn_e \propto n_e^{-\beta}$. We expect β to be positive, i.e., a large volume is occupied by low-density plasma and a small volume contains high-density plasma. The $R_{\rm obs}$ ratios are plotted in Fig. 6 as a function of β for two reasonable ranges of coronal densities $[n_{e,1}, n_{e,2}]$ considered for the power-law distribution. Plausible values of β are 2–4 [30,40].

These examples illustrate that in a *global* coronal picture, the $R_{\rm obs}$ values do not describe "densities" but the *steepness of the density distribution.* While plasma may be present at all densities between the low and the high density limit for the respective triplet, $R_{\rm obs}$ changes from small to large as the density distribution steepens (i.e., as the relative contribution of low-density plasma increases). The transition for a power-law density distribution occurs around $\beta = 3$ (this is a direct consequence of the n_e^2 factor under the integral sign). A slight rearrangement of the distribution of active regions may thus dramatically change $R_{\rm obs}$. Further, again due to the n_e^2 dependence of the line flux, the "inferred density" is *not*

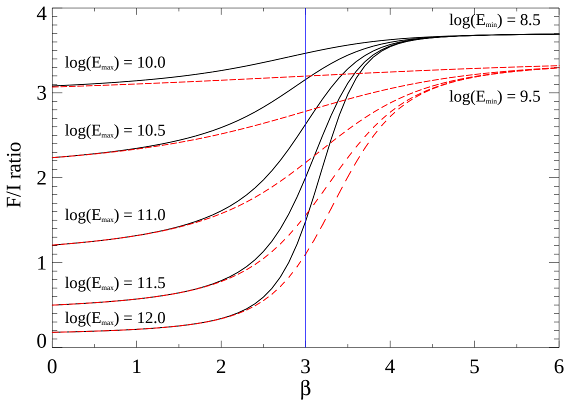

Figure 6. Calculated $R_{\rm obs} = F/I$ flux ratios for the He-like O VII line triplet originating in an inhomogeneous corona with a power-law volume-density distribution (see text for details). The R ratio is plotted as a function of the power-law index β. The different curves are for different ranges of densities at which plasma is assumed to exist (marked by the labels: upper cutoff of the adopted range is given by the labels at left, while labels at right give the lower cutoff). The blue vertical line marks the transition from the low-R to the high-R regime at $\beta = 3$.

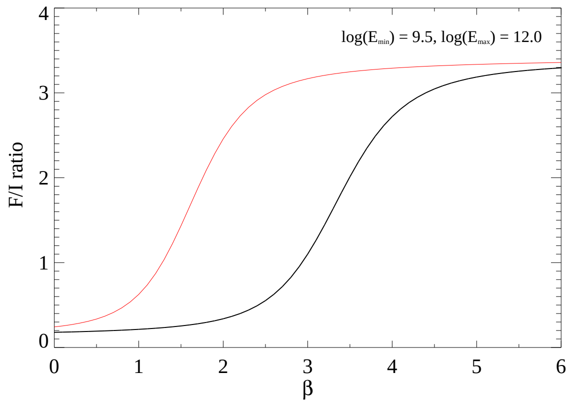

Figure 7. Example illustrating the $R_{\rm obs} = F/I$ ratio as a function of β (bold line), compared with the ratio that corresponds to the volumetric average of all densities considered (thin, red).

and average over the coronal volume. In Fig. 7, the spectroscopically measured R ratios are compared with those corresponding to a *linear* average of all volume contributions (for one example), illustrating that the inferred densities are considerably higher (the R ratios smaller) than the average densities.

The message from this exercise is simple: While a straightforward interpretation of $R_{\rm obs}$ ratios in terms of coronal "density models" clearly leads to problematic results, the $R_{\rm obs}$ ratio contains valuable information on the statistical properties of the state of the hot plasma across the coronal volume. More active main-sequence stars thus appear to maintain flatter density distributions, which could be a consequence of the finite coronal volume: since the latter must be shared by low- and high-density plasmas, the more efficient heating in more active stars (e.g., the increased production of chromospheric evaporation) produces a larger amount of high-density volume, at the cost of the residual low-density volume, thus flattening the distribution and decreasing R. This is the scenario that could be behind the naive perception of a "denser corona". Alternatively, the cutoffs of the density distribution could be shifted to higher values for more active stars, while the slope β is similar (more details are given in Güdel et al., in preparation).

6. Abundances

Elemental abundances in the corona may be an interesting tracer for the coronal heating mechanism since the latter is ultimately responsible for the transport of mass into the corona. X-ray spectroscopy can be used to measure coronal abundance anomalies in magnetically active stars. In the solar corona and in the solar wind, elements with a first ionization potential (FIP) below 10 eV, such as Mg, Si, Ca, Fe, Ni, are overabundant by a factor of a few compared to the photospheric abundances, whereas high-FIP (greater than 10 eV) elements, such as C, N, O, Ar, Ne, are closer to their respective photospheric values.

This abundance pattern has been known as the FIP effect. The chromosphere has the right temperature (4000–10000 K) for high-FIP elements to be predominantly neutral and for low-FIP elements to be considerably ionized. Various models for the FIP effect therefore require the presence of chromospheric electric or magnetic fields that affect ions and neutrals differently (for reviews, see refs. [41] and [42]).

Abundance anomalies in stars have been reported since the *ASCA* and *EUVE* eras but the detected patterns were at variance with solar findings. Very active stars reveal low abundances for all measured elements (e.g., [43,44] for early reviews). High-resolution spectroscopy with *XMM-Newton* and *Chandra* accesses a larger number of individual elements.

A few words of caution are in order, however. The determination of abundances relies on the interpretation of at least a few dozens of strong lines and hundreds of weak lines. Different methods are presently in use to derive abundances, none without intrinsic problems. Methods fitting complete spectra in terms of a number of thermal plasma components and a set of abundances in principle derive a self-consistent picture including the bremsstrahlung continuum, and in particular including calculated weak blends of stronger lines. The drawback of such methods is the large uncertainty in the atomic parameters of many emission lines included in the calculations. Selecting a handful of bright lines to reconstruct an emission measure distribution and the elemental abundances in principle improves the situation, but the line blends and the continuum levels are not described self-consistently, again introducing systematic errors. Uncertain atomic physics parameters even for relatively bright lines produce serious systematic uncertainties regardless of which method is used.

It is therefore rewarding that a number of different investigations based *XMM-Newton* and *Chandra* observations are now converging to somewhat similar results for elemental abundances. In very active stars, an *inverse FIP* effect is regularly found, with low-FIP elements being underabundant relative to high-FIP elements (Fig. 8, see [21,29,45–47,1], and also several further papers in these proceedings), resulting in a large Ne/Fe abundance ratio [45,24]; this effect seems to weaken toward less active stars and may switch over to the solar-type FIP effect in inactive stars [46,48]. The physical cause of this behaviour and its relation to the heating mechanism are presently unclear. Proposals include the presence of numerous Ne-rich flares as occasionally observed in the Sun [49,50], the influence of high-energy electrons that are predominantly present in coronae that show the inverse FIP effect [48], an enhanced He abundance in the corona [24], or "anomalous" photospheric abundances (see discussions in refs. [24,45,46] for further details).

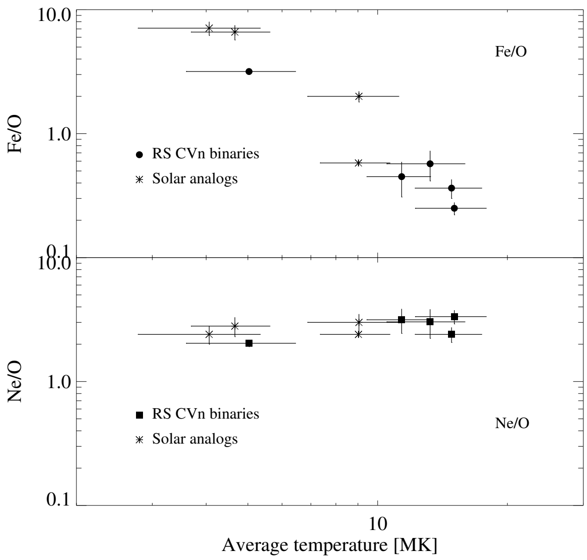

Figure 8. Coronal Fe/O (low FIP/high FIP) and Ne/O (high FIP/high FIP) abundance ratios as a function of the characteristic coronal temperature for several active stars. The ratios are normalized with the respective ratios for the solar photosphere (after [46]).

7. Coronal Shape at Microarcsecond Resolution

Support for thermal and density models of stellar coronae as derived from high-resolution spectroscopy should ultimately come from direct imaging of coronae. Eclipses in binary stars provide powerful means to determine the coronal X-ray structure. Ideally, the eclipsing star is X-ray dark and produces a total stellar eclipse. The distribution of X-ray bright active regions on the eclipsed star should then map uniquely onto the observed light curve as bright areas disappear behind the dark eclipsing limb during eclipse ingress, and reappear during egress.

A system of this kind that happens to contain a young solar analog is α CrB (see [51] for previous observations). It consists of an X-ray dark main sequence A star and a G5 V solar analog orbiting each other in 17.4 d. The inclination is 88.2°, leading to total eclipses of the G star's X-ray corona. The system is of order 500 Myrs old, with the G star's X-ray luminosity ($L_X \approx 6 \times 10^{28}$ erg s^{-1}) exceeding the active Sun's by a factor of about 30 (see ref. [40]

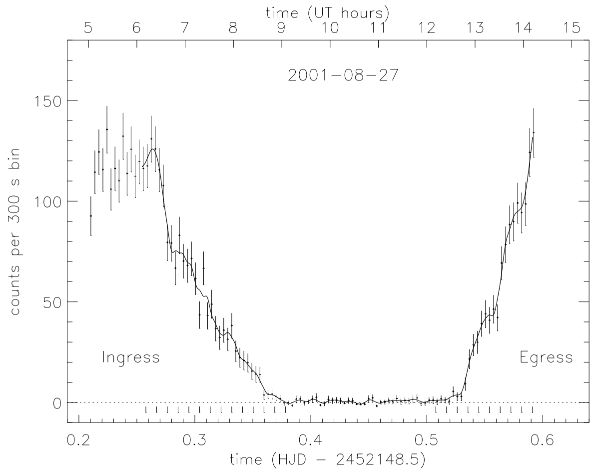

Figure 9. *XMM-Newton* EPIC light curve of the totally eclipsing α CrB system. The total eclipse of the G V star lasts several hours. Plateaus in the ingress and the egress light curves indicate the presence of active regions (after [40]).

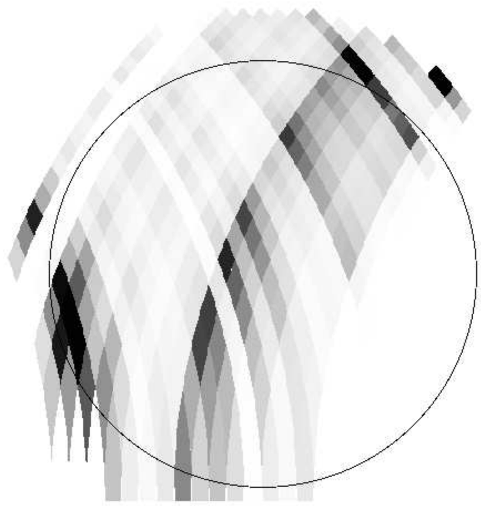

Figure 10. X-ray brightness map of the α CrB secondary star, derived from the light curve shown in Fig. 9. Note several "active regions" (after [40]).

and references therein for further details on the system properties). The light curve observed by *XMM-Newton* is shown in Fig. 9. The ingress and the egress portions of the curve show i) an asymmetric overall shape, ii) various steep declines/increases and plateaus. This points to an inhomogeneous distribution of bright coronal material on the face of the G star, and its concentration in active regions.

The light curve inversion was studied in ref. [40] based on various inversion techniques. One reconstruction of the brightness distribution is shown in Fig. 10. It illustrates the inhomogeneous nature of the X-ray emission. Using estimates for the depth of the emission regions, relatively high densities up to 3×10^{10} cm^{-3} are inferred for some of the active regions. At the same time, the average corona is much hotter (5 MK) than the dominant plasma in the non-flaring Sun. These findings can be accounted for by a simple picture involving interactions of magnetic fields: As the magnetic dynamo increases in strength toward more active stars, the surface filling factor of strong magnetic fields increases, increasing also the volume filling factor of closed loops in the corona. As the magnetic loops are packed closer together than on the Sun, they interact more frequently, producing a higher rate of field annihilation and reconnection, thus generating flares at a higher rate. These energy release events liberate magnetic energy and heat and evaporate chromospheric plasma. One thus expects both a larger average density in the corona and a higher temperature if the flare rate is higher. Increased densities and temperatures both are, in this picture, a natural consequence of a denser packing of magnetic fields in the corona, induced by a more efficient dynamo in stars with more rapid rotation.

8. Spectroscopy and Motion

Spectroscopy is the ultimate means to study plasma motions of all kinds, e.g., turbulent motions, bulk mass flows in magnetic fields, winds and mass ejections, orbital motions, and rotational motions. Mass flows with speeds of several 100 km s^{-1} are expected in flaring magnetic fields. The resulting line shifts could in principle be measured. A marginal but unconfirmed case was described by ref. [22], reporting a short signature of a Doppler blue shift by 100 km s^{-1} in the Ne X line before a flare. No positive reports are available from other flare observations with *XMM-Newton* and *Chandra*. This is perhaps not completely surprising. Although mass upflows are expected during the early flare episodes, i) most flares occur, for geometric reasons, close to the stellar limb, so that the velocity component along the line of sight is often relatively small.

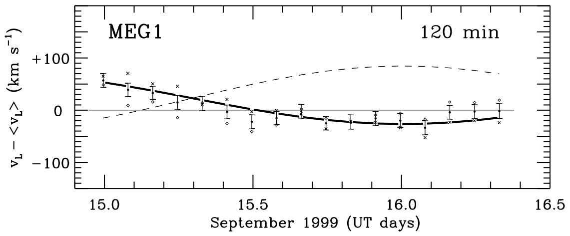

Figure 11. Doppler displacement of the Ne X line in the HR 1099 *Chandra* X-ray spectrum compared to expectation if the source were on the primary K star (bold line) or on the secondary G star (thin line). (After [22].)

ii) The highest evaporative flow velocities are expected in the early phase of the flare when the signal is usually weak and superimposed on the emission of the more steady corona of the star as a whole. iii) At stages when the emission measure of a flare is large, most of the plasma is already stationary, and this plasma outshines the moving component.

Orbital motion has successfully been detected in HR 1099 by the same authors [22]. Fig. 11 shows the velocity displacement of the Ne X line during a long *Chandra* observation of this system, together with the calculated expected Doppler shift of the K star (bold) and the companion G star (dashed). This result unambiguously relates most of the observed X-ray emission with the subgiant K star. Since the emission is rotationally modulated ([21] and references therein) with the peak occurring when the K star is in front, the X-ray activity seems to predominate on the K star hemisphere facing away from the companion star.

If both stars in a binary contribute to the X-ray emission, then periodic line *broadening* is expected instead of line shifts. The two components in the YY Gem dMe+dMe binary system show an equal X-ray luminosity level, as suggested by similar primary and secondary X-ray eclipses [9,30]. Periodic line broadening with a period of one-half of the rotation period was indeed found, with the correct velocity amplitude [30].

9. Conclusions

High-resolution X-ray spectroscopy has opened completely new windows to the study of coronae of cool stars. For the first time, we have detailed routine access to numerous physical processes and properties of magnetically confined stellar plasmas. Not only can the temperature structure be studied in much more detail than before, the multitude of individual spectral lines also allow us to determine the composition of coronae, measure densities and therefore pressures, infer mass motions, or locate the observed emission.

A few words of caution are nevertheless in order. The objects in question are highly complex plasma-physical systems, dominated by continuously changing and frequently unstable magnetic fields, by explosive heating mechanisms, mass motions, and various cooling processes. Yet, we are interpreting - in most cases - single integrated spectra. The number of parameters required to approximately describe the state of a particular corona is beyond the reach of any spectroscopic detector that lacks angular resolution. The complex time-dependent density structure of a corona that leads to a singular time-averaged R ratio in the spectrum illustrates the degeneracy. Further complexities come to mind: The "coronal composition" may be different in different areas on a star, and perhaps an inverse FIP effect predominates in high-density, hot active regions, while a normal FIP effect governs cooler plasma. The FIP bias may even be time-variable in individual regions, but spectroscopy will not resolve this due to its spatial averaging. What we perceive as steady emission, to be interpreted with a single high-resolution X-ray spectrum, may in fact be the superposition of large numbers of explosive events, each with its own (time-variable!) abundance pattern, with its own time-variable emission measure distribution, and with its own time-dependent density development. No spectrum will ever disentangle this complexity. Luckily so. The physical understanding of "stellar coronae" is not founded in the ever increasing description of smaller and smaller details, but in the recognition of global trends that come to light by investigation of stars as a whole and by comparing stars with different properties. There is need to study coronal systems as *statistical ensembles* of smaller, unresolvable building blocks that vary in time, in density, in composition, in temperature, etc. Reading the statistical properties from spectra and light curves will greatly help interpret the ensemble of physical processes that occur at any given time at many places in a stellar corona.

REFERENCES

1. Huenemoerder, D. P. 2002, these proceedings
2. Neupert, W. M. 1968, ApJ, 153, L59
3. Hawley, S. L., Fisher, G. H., Simon, T., *et al.* 1995, ApJ, 453, 464
4. Güdel, M., Benz, A.O., Schmitt, J. H. M. M., & Skinner, S. L. 1996, ApJ, 471, 1002
5. Güdel, M., Audard, M., Skinner, S. L., & Horvath, M. I. 2002a, ApJ, 580, L73
6. Güdel, M., Audard, M., Smith, K. W., *et al.* 2002b, ApJ, 577, 371
7. Gabriel, A. H., & Jordan, C. 1969, MNRAS, 145, 241
8. Porquet, D., Mewe, R., Dubau, J., *et al.* 2001, A&A, 376, 1113
9. Stelzer, B., Aschenbach, B., Audard, M., *et al.* 2002, A&A, 392, 585
10. Osten, R., Ayres, T. R., Brown, A., *et al.* 2002, ApJ, in press
11. Lin, R. P., Schwartz, R. A., Kane, S. R., *et al.* 1984, ApJ, 283, 421
12. Audard, M., Güdel, M., & Guinan, E. F. 1999, ApJ, 513, L53
13. Audard, M., Güdel, M., Drake, J. J., & V. Kashyap, V. L. 2000, ApJ, 541, 396
14. Kashyap, V. L., Drake, J. J., Güdel, M., & Audard, M. 2002, ApJ, 580, 1118
15. Güdel, M., Audard, M., Kashyap, V. L., *et al.* 2003a, ApJ, in press
16. Kashyap, V. L., Drake, J. J., Güdel, M., & Audard, M. 2003, Adv. Space Res., in press
17. Schrijver, C. J., Mewe, R., & Walter, F. M. 1984, A&A, 138, 258
18. Brinkman, A. C., *et al.* 2000, ApJ, 530, L111
19. Canizares, C. R., *et al.* 2000, ApJ, 539, L41
20. Audard, M., Behar, E., Güdel M., *et al.* 2001a, ApJ, 365, L329
21. Audard, M., Güdel, M., & Mewe, R. 2001b, A&A, 365, L318
22. Ayres, T. R., Brown, A., Osten, R. A., *et al.* 2001, ApJ, 549, 554
23. Behar, E., Cottam, J., & Kahn, S. M. 2001, ApJ, 548, 966
24. Drake, J. J., Brickhouse, N. S., Kashyap, V., *et al.* 2001, ApJ, 548, L81
25. Huenemoerder, D. P., Canizares, C. R., & Schulz, N. S. 2001, ApJ, 559, 1135
26. Mewe, R., Raassen, A. J. J., Drake, J. J., *et al.* 2001, A&A, 368, 888
27. Phillips, K. J. H., Mathioudakis, M., Huenemoerder, D. P., *et al.* 2001, MNRAS, 325, 1500
28. Raassen, A. J. J., Mewe, R., Audard, M., *et al.* 2002, A&A, 389, 228
29. Güdel, M., Audard, M., Briggs, K., *et al.* 2001a, A&A, 365, L336
30. Güdel, M., Audard, M., Magee, H., *et al.* 2001b, A&A, 365, L344
31. Feldman, U., Laming, J. M., & Doschek G. A. 1995, ApJ, 451, L79
32. Cargill, P. J. 1994, ApJ, 422, 381
33. Drake, J. J., Peres, G., Orlando, S., *et al.* 2000, ApJ, 545, 1074
34. Linsky, J. L., Ayres, T. R., Brown, A., & Osten, R. A. 2002, Astron. Nachrichten, 323, 321
35. Maggio, A., Drake, J. J., Kashyap, V., *et al.* 2002, in Stellar Coronae in the Chandra and XMM-Newton Era, eds. F. Favata & J. J. Drake (San Francisco: ASP), 57
36. Ness, J.-U., Mewe, R., Schmitt, J. H. M. M., *et al.* 2001, A&A, 367, 282
37. Ness, J.-U., Schmitt, J. H. M. M., Burwitz, V., *et al.* 2002, A&A, 387, 1032
38. Ness, J.-U., Schmitt, J. H. M. M., Burwitz, V., *et al.* 2002, A&A, 394, 911
39. Kastner, J. H., Huenemoerder, D. P., Schulz, N. S., *et al.* 2002, ApJ, 567, 434
40. Güdel, M., Arzner, K., Audard, M., & Mewe, R. 2003b, A&A, submitted
41. Feldman, U. 1992, Phys. Scripta, 46, 202
42. Hénoux, J.-C. 1995, Adv. Space Res., 15, 23
43. White, N. E. 1996, in 9th Cambridge Workshop on cool stars, stellar systems, and the Sun, ed. R. Pallavicini & A. K. Dupree (San Francisco:ASP), 193
44. Drake, S. A. 1996, in 6th Annual Astrophysics Conference, Maryland, ed. S. S. Holt & G. Sonneborn, 215
45. Brinkman, A. C., *et al.* 2001, A&A, 365, L324
46. Audard, M., Güdel, M., Sres, A., *et al.* 2003, A&A, in press
47. Schmitt, J. H. M. M. 2002, these proceedings
48. Güdel, M., Audard, M., Sres, A., *et al.* 2002c, in Stellar Coronae in the Chandra and XMM-Newton Era, eds. F. Favata & J. J. Drake (San Francisco: ASP), 497
49. Schmelz, J. T. 1993, ApJ, 408, 373
50. Shemi, A. 1991, MNRAS, 251, 221
51. Schmitt, J. H. M. M., & Kürster, M. 1993, Science, 262, 215

ACKNOWLEDGEMENTS

I thank Marc Audard for helpful discussions during the preparation of this paper; figures were generously provided by Jan-Uwe Ness, Tom Ayres, and Marc Audard. Work at PSI was supported by the Swiss National Science Foundation (grant 2000-058827).